

to the dipole vibrations of the film atoms polarized parallel to the substrate. The field of such a dipole penetrates into the metal and drags the conduction electrons. A reduction in the conductivity of the metal substrate enhances the transfer of energy from the dipole vibrations of the insulator "ions" to the metal and it shifts and broadens the low-frequency emission band.

Determination of the Raman spectra indicated that the influence of the conduction electrons in the metal substrate on the insulator polaritons in such sandwiches decreases rapidly on increase of the polariton wave vector. When this wave vector rises from 10^3 to 10^5 cm^{-1} , the shift and broadening of the low-frequency emission peak practically disappear.

The authors regard it as their pleasant duty to thank N.I. Mel'nik for recording the Raman spectra, and to Prof. V.M. Agranovich for his interest and discussion of the results obtained.

¹V. M. Agranovich and T. A. Leskova, *Fiz. Tverd. Tela (Leningrad)* **16**, 1800 (1974) [*Sov. Phys. Solid State* **16**, 1172

(1974)].

²G. N. Zhizhin, O. I. Kapusta, M. A. Moskaleva, V. G. Nazin, and V. A. Yakovlev, *Fiz. Tverd. Tela (Leningrad)* **17**, 2008 (1975) [*Sov. Phys. Solid State* **17**, 1313 (1975)].

³V. A. Yakovlev, Candidate's Thesis, Institute of Spectroscopy, Academy of Sciences of the USSR, Moscow, 1976.

⁴E. A. Vinogradov, G. N. Zhizhin, A. G. Mal'shukov, and V. I. Yudson, *Solid State Commun.* **23**, 915 (1977).

⁵E. A. Vinogradov, G. N. Zhizhin, and A. G. Mal'shukov, *Zh. Eksp. Teor. Fiz.* **73**, 1480 (1977) [*Sov. Phys. JETP* **46**, 778 (1977)].

⁶D. L. Stierwalt and R. F. Potter, "Emission studies," in *Semiconductors and Semimetals* (ed. by R. K. Willardson and A. C. Beer), Vol. 3, Optical Properties of III-V Compounds, Academic Press, New York, 1967, p. 71 (Russ. Transl. Mir, M., 1970, p. 80).

⁷K. Hisano, Y. Okamoto, and O. Matumura, *J. Phys. Soc. Jpn.* **28**, 425 (1970).

⁸E. A. Vinogradov, G. N. Zhizhin, N. N. Mel'nik, and O. K. Filippov, *Fiz. Tverd. Tela (Leningrad)* **18**, 2647 (1976) [*Sov. Phys. Solid State* **18**, 1544 (1976)].

⁹K. L. Kliewer and R. Fuchs, *Phys. Rev.* **150**, 573 (1966); R. Fuchs, K. L. Kliewer, and W. J. Pardee, *Phys. Rev.* **150**, 589 (1966).

¹⁰J. M. Ziman, *Principles of the Theory of Solids*, Cambridge University Press, 1964 (Russ. Transl., Mir, M., 1966, p. 282).

Translated by A. Tybulewicz

Study of orientational ordering of uniaxial liquid crystal by Raman-scattering spectroscopy

V. F. Shabanov, E. M. Aver'yanov, P. V. Adomenas, and V. P. Spiridonov

Physics Institute, Siberian Division, USSR Academy of Sciences

(Submitted 26 June 1978)

Zh. Eksp. Teor. Fiz. **75**, 1926-1934 (November 1978)

A new procedure is proposed for the study of the orientational molecular ordering in uniaxial liquid crystals of *A*-smectic, nematic, and cholesteric type by laser Raman spectroscopy. Expressions are obtained from which to determine the coefficients of the expansion of the orientational molecular distribution function in powers of the experimental degrees of depolarization of the Raman scattering lines. The orientational molecular order in the nematic phase of methoxyamyltolane is investigated experimentally. It is shown that the anisotropy of the local field influences strongly the experimental results.

PACS numbers: 61.30.Eb, 61.30.Gd, 78.30.Cp

1. INTRODUCTION

Combining the various types of orientational and translational molecular orders in the mesophase results in a large assortment of possible liquid-crystal structures.¹ Those of them which are optically uniaxial are the *A*-smectic, nematic, and cholesteric liquid crystals. For a quantitative description of the orientational ordering of the molecules in each of the indicated types of liquid crystals, we use the orientational distribution function $F(\varphi, \theta, \psi)$, which yields the probability of finding the orientation of the molecule in a small

solid angle $d\Omega$ near the corresponding Euler angles φ , θ , and ψ (Ref. 2). These angles define the orientation of the molecular coordinate system relative to the laboratory frame. In nematic and *A*-smectic liquid crystals, the z axis is chosen to coincide with the director \mathbf{r} , and the x and y axes are in a plane perpendicular to it. In the quasinematic layer of the planar texture of a cholesteric liquid crystal, the z axis coincides with the director \mathbf{r}_c of the layer, the x axis lies in the plane of the layer, and y is perpendicular to the layer. X-ray structure data^{1,3,4} show that the directions \mathbf{r} and $(-\mathbf{r})$ in nematics and *A*-smectics are equivalent. The same

holds for r_c and $(-r_c)$ in quasinematic layers of cholesterics.

Next, as follows from experiment, the types of liquid crystals considered here are locally uniaxial, and the projections of the long axes of the molecules on the xy planes of the laboratory frames chosen above are randomly distributed. Finally, most liquid-crystal molecules are cylindrical in shape and the molecules in the mesophase rotate around their long axes.^{2,5}

With the foregoing taken into account, the functional dependence of F is determined only by the angle θ between the long axis of the molecule and the direction of r . In this approximation, F describes the orientational distribution of the long molecular axes in the mesophase and can be represented in the form of an expansion in even Legendre polynomials $P_l(\cos\theta)$ (Ref. 6):

$$F(\theta) = \frac{1}{2} + \frac{3}{2} \langle P_2 \rangle P_2 + \frac{5}{2} \langle P_4 \rangle P_4 + \dots, \quad (1)$$

where

$$P_2 = \frac{1}{2}(3 \cos^2 \theta - 1), \quad (2)$$

$$P_4 = \frac{1}{8}(35 \cos^4 \theta - 30 \cos^2 \theta + 3).$$

The angle brackets denote thermal averaging.

The coefficients of the expansion of $F(\theta)$ can be determined from the experimental data. To find $\langle P_2 \rangle$ in nematics and A -smectics there are a number of suitable physical methods.⁵ For the determination of $\langle P_2 \rangle$ of cholesteric liquid crystals it was proposed to use nuclear magnetic resonance,⁷ refractometry,⁸ and circular dichroism.⁹ The possibility of obtaining $\langle P_4 \rangle$ for A -smectic and nematics was recently demonstrated¹⁰ by using luminescence¹⁰ and Raman spectroscopy (RS).^{6,11,12} No attempts have been made so far to determine the values of $\langle P_4 \rangle$ of cholesteric liquid crystals by some physical method.

Raman spectroscopy makes it possible to find both $\langle P_2 \rangle$ and $\langle P_4 \rangle$ for any valent bond in the molecule, including the end groups. The last circumstance is particularly important when it comes to separate the role of conformational molecular changes in the formation of the mesophase.¹³

The values of $\langle P_4 \rangle$ obtained from the degree of depolarization of the lines of spontaneous Raman scattering (SpRS) for certain objects do not agree with the theoretical data even in sign, especially near the point T_f of the phase transition into a isotropic liquid.^{6,14} It must be emphasized that $\langle P_2 \rangle$ and $\langle P_4 \rangle$ are fundamental quantities that serve as criteria for the correctness of some theoretical model or another. The experimental data were reduced in the cited papers without allowance for two aspects of the problem of the local field: the anisotropy of the local field of the light wave in the liquid crystal, and the influence of the anisotropy of the intermolecular-interaction potential on the change of the properties of the molecule in the liquid crystal compared with the isotropic phase. The importance of the anisotropy of the local field of the light wave in optical experiments was demonstrated by us earlier.^{15,16} The need for taking into account the changes of the molecular properties in an anisotropic medium was pointed out

in a number of papers.^{10,17,18}

In this paper we obtain expressions for the determination of the values of $\langle P_2 \rangle$ and $\langle P_4 \rangle$ from SpRS data on A -smectic, nematic, and cholesteric liquid crystals, with account taken of the anisotropy of the local field (2). We describe the experimental setup and the procedures that can be used to determine the degree of depolarization (3), and present the results of a study of the orientational order in the nematic liquid crystal methoxyamyltolane (4).

2. ORIENTATIONAL ORDER IN UNIAXIAL LIQUID CRYSTALS AND DEGREE OF DEPOLARIZATION OF RAMAN SCATTERING LINES

We consider Raman scattering (RS) of light by an intramolecular vibration of frequency ν_i in the liquid-crystal laboratory frame defined above. Within the framework of Placzek's polarizability theory¹⁹ with allowance for the local field in the condensed medium,²⁰ the intensity of the Stokes component of light of polarization j scattered by one molecule into a solid angle $d\Omega$ and observed perpendicular to the j axis is²¹

$$dJ_{ij} = J_{ij}^2 \frac{n_i^2}{n_i} f_{ij}^2 \frac{2\pi^2 (v_0 - \nu_i) h (\alpha'_{ji})^2 J_{0i} d\Omega}{\mu c^3 \nu_i [1 - \exp(-h\nu_i/kT)]}. \quad (3)$$

Here ν_0 is the frequency of the exciting light, polarized along the i axis; f_{ij} are the components of the light-wave local-field tensor, which is diagonal in the frame under consideration^{8,15} and connects the macroscopic field with the field that acts on the molecule, $E_i^T = f_{ij} E_j$; n_i , n_j^* are the refractive indices of the incident and scattered rays, respectively; μ is the reduced mass of the oscillator; c , h , k , and T are the speed of light, Planck's constant, Boltzmann's constant, and the absolute temperature; α'_{ji} is the derivative of the molecular-polarizability tensor components with respect to the normal coordinate; J_{0i} is the intensity of the exciting light.

When the scattered radiation is observed at an angle Φ to the direction of the j axis, expression (3) must be multiplied from the right by $\sin^2 \Phi$. In the studies made to data of spontaneous Raman scattering in liquid crystals, they used for the intensity a formula obtained from (3) by putting $n_i = n_j^*$ and $f = (\bar{n}^2 + 2)/3$, i.e., by neglecting the optical anisotropy of the medium and the anisotropy of the local-field tensor. At low intensities of the incident light the scattering of different molecules is not coherent. The total intensity in a given direction is then

$$dJ_{ij}^{\text{tot}} = \sum_{\sigma=1}^N dJ_{ij}^{(\sigma)} = N \langle dJ_{ij}^{(\sigma)} \rangle, \quad (4)$$

where $dJ_{ij}^{(\sigma)}$ is given by expression (3), N is the number of molecules that take part in the scattering, and the angle brackets denote averaging over the orientations of the different molecules.

For cholesteric liquid crystals, the averaging in (4) is within the limits of the quasinematic layer. It is clear from (4) that the distribution of the intensity over the components in the scattering tensor of the liquid crystal depends on the character of the averaging, i.e., it re-

flects the properties of the long-range orientational order in the liquid crystal. In the intrinsic coordinate system, the tensor of the derivative of the molecular polarizability is diagonal. When account is taken of the singularities, noted in Sec. 1, of the orientational order in the *A*-smectic, nematic, and cholesteric liquid crystals, the result is that the RS lines have in the macroscopic intensity tensor only four independent components. In the case of cylindrical symmetry of the normal vibration, e.g., for the $C \equiv C$ bond, we can obtain²¹

$$\begin{aligned} \langle (\alpha_{xx}')^2 \rangle &= (\gamma_{33}')^2 [R^2 + R(1-R)\langle s^2 \rangle + 1/8(1-R)^2\langle s^4 \rangle], \\ \langle (\alpha_{zz}')^2 \rangle &= (\gamma_{33}')^2 [1 - 2(1-R)\langle s^2 \rangle + (1-R)^2\langle s^4 \rangle], \\ \langle (\alpha_{xy}')^2 \rangle &= (\gamma_{33}')^2 \cdot 1/8(1-R)^2\langle s^4 \rangle, \\ \langle (\alpha_{xz}')^2 \rangle &= (\gamma_{33}')^2 \cdot 1/2(1-R)^2[\langle s^2 \rangle - \langle s^4 \rangle]. \end{aligned} \quad (5)$$

Here γ_{33}' is the component of the molecular-system polarizability-tensor derivative in the coordinate system along the symmetry axis of the bond,

$$R = \gamma_{11}' / \gamma_{33}', \quad \langle s^2 \rangle = \langle \sin^2 \theta \rangle, \quad \langle s^4 \rangle = \langle \sin^4 \theta \rangle.$$

In the present paper, the experimental procedure proposed for nematics and *A*-smectics differs from those used previously^{8,11,14} (see Fig. 1 below). We measure in the experiment the degree of depolarization $\rho = J_{xz} / J_{xx}$ of the RS lines at two orientations of the sample optical axis relative to the scattering plane *YZ*. In the first case (a) the optical axis of the crystal lies in the scattering plane and makes an angle ε with the *Z* axis. In the second case (b) the optical axis of the crystal is parallel to the *X* axis of the coordinate system of the instrument at the same arrangement of the cell as in case (a). The intensity vector of the exciting beam is parallel in both cases to *X*. The optimal angle of inclination of the cell with plane-parallel faces is 11°, and 5° for a cell with a hemisphere.

When account is taken of the effects of reflection and refraction of the scattered radiation by the boundary between the liquid crystal and the glass,²¹ the expressions for the experimentally observed degrees of depolarization take the form

$$\rho_1 = \frac{J_{xz}(a)}{J_{xx}(a)} = \frac{f_{xz}^2(n_e+n)^2[A\langle s^4 \rangle + B\langle s^2 \rangle]}{f_{zz}^2(n_e+n)^2[C\langle s^4 \rangle + D\langle s^2 \rangle + E]}, \quad (6)$$

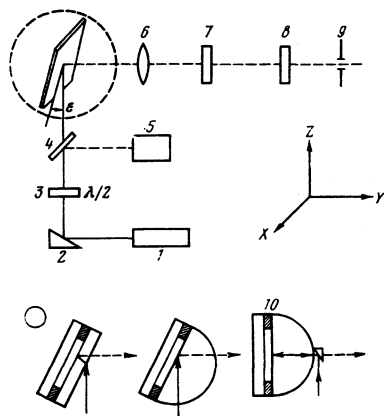


FIG. 1. Experimental setup for the measurement of the degrees of depolarization of Raman lines of liquid crystals. The lower part shows in detail a diagram of the cell in the dashed circle of the upper part.

$$\rho_2 = \frac{J_{xz}(b)}{J_{xx}(b)} = \frac{f_{xz}^2(n_e+n)^2[\langle s^2 \rangle - \langle s^4 \rangle]}{f_{zz}^2(n_e+n)^2[2\langle s^2 \rangle - F\langle s^2 \rangle + G]}. \quad (7)$$

In (6) and (7)

$$A = 1/8(1 - 5 \cos^2 \varepsilon'), \quad B = 1/2 \cos^2 \varepsilon', \quad C = 3/8, \quad (8)$$

$$D = R/(1-R), \quad E = D^2, \quad F = 4/(1-R), \quad G = 2/(1-R)^2,$$

ε' is the angle of incidence of the extraordinary ray on the boundary between the liquid crystal and the glass; n_e and n_o are the extraordinary and ordinary refractive indices of the liquid crystal at the given temperature, and n is the refractive index of the cell material.

In the case of an isotropic phase, when $n_e = n_o$, $f_{xx} = f_{zz}$, $\langle s^2 \rangle = 2/3$ and $\langle s^4 \rangle = 8/15$, formulas (6) and (7) take the well known form²²

$$\rho_1 = \rho_2 = \frac{(1-R)^2}{8R^2 + 4R - 3}. \quad (9)$$

Using now the reduced degrees of depolarization

$$\begin{aligned} \rho_1' &= \frac{f_{xz}^2(n_e+n)^2}{f_{zz}^2(n_e+n)^2} \rho_1 = \lambda \rho_1, \\ \rho_2' &= \lambda^{-1} \rho_2, \end{aligned} \quad (10)$$

we readily obtain from (2) and (6), and (7) the following expressions for $\langle P_2 \rangle$ and $\langle P_4 \rangle$:

$$\langle P_2 \rangle = 1 - 3/2 \langle s^2 \rangle, \quad (11)$$

$$\langle P_2 \rangle = 1 - \frac{3/2[\rho_1' E(1+2\rho_2') + \rho_2' G(A - \rho_1' C)]}{(A - \rho_1' C)(1 + \rho_2' F) + (1 + 2\rho_2')(B - \rho_1' D)}, \quad (11a)$$

$$\langle P_2 \rangle = 3/8 \langle s^4 \rangle - 5/2 \langle s^2 \rangle + 1, \quad (12)$$

$$\begin{aligned} \langle P_4 \rangle &= 1 - \frac{3/8}{(A - \rho_1' C)(1 + \rho_2' F) + (1 + 2\rho_2')(B - \rho_1' D)} \\ &\times \{\rho_1' E[1 + \rho_2'(16 - 7F)] + \rho_2' G[8A + 7B - \rho_1'(8C + 7D)]\}. \end{aligned} \quad (12a)$$

Formulas (11a) and (12a) enable us to obtain $\langle P_2 \rangle$ and $\langle P_4 \rangle$ in nematic and *A*-smectic liquid crystals from the Raman scattering data.

It is difficult to use this method for cholesteric liquid crystals because it is necessary to take into account the effect of the helical character of the structure along the optical axis on the polarization properties of the exciting light. In addition, there is no exact solution of Maxwell's equations for oblique light incidence on the optical axis.⁵ It is proposed therefore to use a 180° procedure for cholesteric liquid crystals with "fingerprint" texture. In such a texture the quasinematic layers are perpendicular to the cell walls and the optical axis of the sample is parallel to the walls.

To obtain 180° scattering, we use a cell with rotating prism (10 in Fig. 1 below), with an edge on the order of 1 mm. The optical axis of the sample is parallel to the *Z* axis of the instrument, and the incident and scattered light rays are perpendicular to the *XZ* plane of the cell walls. Using (3), where the subscripts *ij* pertain now to the coordinate system of the instrument, as well as formulas (5) for the coordinate system of the director r_s in the layer, we obtain

$$\rho_3 = \frac{J_{zx}}{J_{zz}} = \frac{f_{zx}^2(n_e+n)^2[a\langle s^2 \rangle + b\langle s^4 \rangle]}{f_{zz}^2(n_e+n)^2[c\langle s^4 \rangle + d\langle s^2 \rangle + e]}, \quad (13)$$

$$\rho_4 = \frac{J_{xz}}{J_{xx}} = \frac{f_{xz}^2(n_e+n)^2[a\langle s^2 \rangle + b\langle s^4 \rangle]}{f_{xx}^2(n_e+n)^2[k\langle s^4 \rangle + m\langle s^2 \rangle + g]} \quad (14)$$

where

$$a=4, b=-3, c=6, d=16R/(1-R), e=16R^2/(1-R)^2, \\ k=9/4, m=2(R+3)/(R-1), g=2(3R^2+2R+3).$$

In the case of an isotropic phase formulas (13) and (14) go over into (9). In the derivation of (13) and (14) it was assumed that the cholesteric is locally uniaxial² and the diameter of the laser beam exceeds the pitch of the helix, and $\langle(\alpha'_{ij})^2\rangle$ in (3) was further averaged over the pitch of the helix.

From (11)–(14) we have

$$\langle P_2 \rangle = 1 - \frac{3/2 [\rho'_s e (\rho'_s k + b) + \rho'_s g (b - \rho'_s c)]}{(\rho'_s c - b) (\rho'_s m - a) + (a - \rho'_s d) (\rho'_s k - b)}, \quad (15)$$

$$\langle P_4 \rangle = 1 - \frac{3/8}{(\rho'_s c - b) (\rho'_s m - a) + (a - \rho'_s d) (\rho'_s k - b)},$$

$$\times \{ \rho'_s e [\rho'_s (7m + 8k) - (7a + 8b)] + \rho'_s g [(7a + 8b) - \rho'_s (7d + 8c)] \}, \quad (16)$$

where

$$\rho'_s = \frac{f_{zz}^2 (n_o + n)^2}{f_{xx}^2 (n_e + n)^2}; \quad \rho_s = U \rho_s, \quad \rho'_s = \frac{\rho_s}{U}.$$

Thus, to determine the quantities $\langle P_2 \rangle$ and $\langle P_4 \rangle$ in the liquid crystals of the type considered above it is necessary to measure quantitatively the degrees of depolarization of the Raman scattering lines.

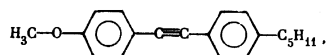
3. EXPERIMENTAL PROCEDURE

A diagram of the experimental setup is shown in Fig. 1. To excite the Raman spectrum we used an LG-38 helium-neon laser ($\lambda_0 = 633$ nm) operating in the one-mode regime and having a system for automatic control of the power (35 mW, 1 in Fig. 1). To verify the influence of the wavelength of the exciting radiation on the degree of depolarization ρ , the measurements were made also with an argon laser ($\lambda_0 = 454$ and 515 nm) whose power was constantly monitored. At an exciting beam power higher than 60–70 mW, local heating of the nematic liquid crystal becomes noticeable. A half-wave plate 3 was placed past the turning prism 2 to rotate the plane of polarization of the laser beam. Part of the laser signal was next diverted by plate 4 to the attachment 5 that monitored the power. The scattered light was resolved into components by analyzer 7. To equalize the losses of the differently polarized Raman components in the instrument, the plane-polarized beam was transformed, after passing through wedge 8, into a circularly polarized one. The height and width of the exit slit 9 of the DFS-24 monochromator was set at their optimal values.

The liquid crystal was oriented by the procedure of Ref. 23. The quality of the sample was monitored with an MIN-8 polarization microscope. The sample thickness was varied in the range from 6 to 150 μm . Two types of cells, shown in Fig. 1 were used. The cell with the plane-parallel plates is more compact and easier to construct. The second construction is convenient for use with a low-power laser, since it lowers substantially the reflection losses of the exciting beam. The cell with the liquid crystal was placed in a thermostatically controlled cuvette in which the temperature was maintained constant within 0.1°. To determine ρ we used the integrated intensities of the Raman lines.

4. ORIENTATIONAL MOLECULAR ORDER IN METHOXYAMYL TOLANE

To find $\langle P_2 \rangle$ and $\langle P_4 \rangle$ we must know the characteristic R of the normal intramolecular vibration. In the isotropic phase, R can be determined from formula (9), but its value can change on going to the mesophase. This is attested to by the results of a number of studies.^{10,17,18} As is clear from (8), the most suitable for our present problem are oscillations with $R \ll 1$. Then a change of even several dozen per cent in R following the transition into the mesophase will not affect the result noticeably. This condition is satisfied by the vibrations of the triple C \equiv N and C \equiv C bonds. The choice of the C \equiv C bond is preferable because of its low sensitivity to the intermolecular interactions. We have therefore chosen methoxyamyltolane (MOAT) as the object of the investigation:



which has a nematic phase in the interval 44–57°C. The vibrations of the C \equiv C bond has a frequency 2219 cm^{-1} and conforms with the long axis of the molecule.

The instrumental distortions apart, the degree of depolarization depends on at least three additional factors: the scattering due to rays multiply reflected from the inner walls of the cell, the multiple scattering due to reradiation of the light by the molecules in the interior of the liquid-crystal layer, and the thermal local fluctuations of the director. The first of these effects plays a noticeable degree in 180° scattering and can be decreased by the procedure described here. In addition,

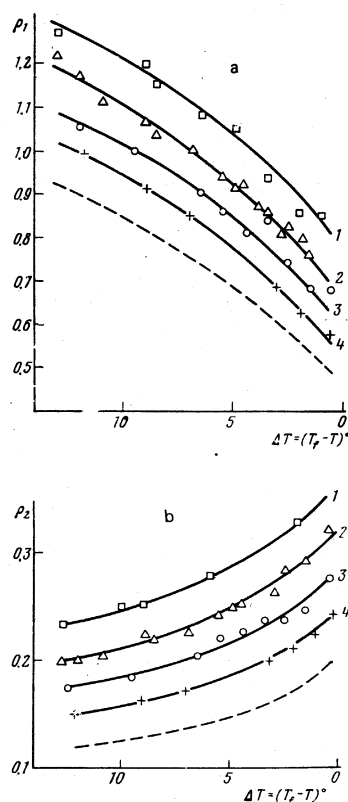


FIG. 2. Dependences of ρ_1 (a) and ρ_2 (b) of the liquid crystal MOAT in the nematic phase on the temperature ($^{\circ}\text{C}$) at various sample thicknesses d : 1) 150, 2) 100, 3) 60, and 4) 35 μm . T_f is the temperature of the transition to the isotropic phase. The dashed line corresponds to the values of ρ_1 at $d = 0$. The data were obtained with a helium-neon laser.

the liquid-crystal section from which the scattered radiation is gathered is longer in this case. The influence of multiple scattering is eliminated in part by extrapolating to zero sample thickness, $d=0$, the experimentally obtained $\rho_i(d)$ as a function of the sample thickness. Figures 2(a) and 2(b) show the experimental changes of ρ_1 and ρ_2 of the MOAT liquid crystal at various sample thicknesses, obtained in helium-neon laser illumination.

The use of an argon laser made it possible to measure ρ_1 and ρ_2 at different exciting-beam wavelengths. The values of ρ'_i obtained with different lasers are equal for equal sample thicknesses. The values of ρ'_i at $d=6 \mu\text{m}$ obtained with an argon laser agree within the limits of experimental accuracy with those obtained by extrapolation to zero thickness (Fig. 2) with a helium-neon laser. This is due to the relatively large distance to the lowest electronic transition, whose band edge in MOAT lies in the 340 nm region. The agreement between the plots of ρ_i in Figs. 2 and 3 points to a small influence of the boundary conditions at the cuvette walls on the bulk properties of the sample at $d=6 \mu\text{m}$ and to a weak dependence of the multiple scattering on λ_0 . Consequently, in future experiments it is advisable to use samples 5–10 μm thick in any of the cells shown in Fig. 1.

The values of $\langle P_2 \rangle$ and $\langle P_4 \rangle$ were calculated from formulas (8) and (10)–(12a). The refractive indices of MOAT were taken from the paper of Labrune and Bresse.²⁴ The value of R was obtained from (9) using the spectra of the isotropic phase, and is equal to 0.045 ± 0.015 . The components of the tensor f_{ii} were obtained by the method used by us previously.¹⁵ The calculation details are given elsewhere.²¹ The temperature dependences of the parameters $\langle P_2 \rangle$ and $\langle P_4 \rangle$ are shown in Fig. 4. A smooth decrease of the degree of orientational order is observed in the nematic phase when the point of phase transition into the isotropic liquid is approached. The values of $\langle P_2 \rangle$ and $\langle P_4 \rangle$ increase when account is taken of the anisotropy of the tensor f of the local light-wave field. The relative changes are particularly substantial for $\langle P_4 \rangle$ and amount to 100–150% near the transition. When R is varied, the values of

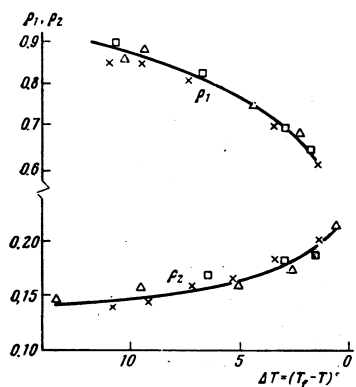


FIG. 3. Temperature dependences of ρ_1 and ρ_2 at exciting-light wavelengths $\lambda_0 = 515 \text{ nm}$ (\square) and 454 nm (\triangle) for a cell with plane-parallel faces and $\lambda_0 = 515 \text{ nm}$ (\times) for a cell with hemisphere; $d = 6 \mu\text{m}$.

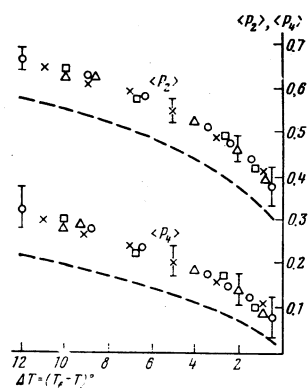


FIG. 4. Temperature dependences of the parameters $\langle P_2 \rangle$ and $\langle P_4 \rangle$ in MOAT under various experimental conditions: \circ) $\lambda_1 = 633 \text{ nm}$, $d = 0$; \square) $\lambda_0 = 515 \text{ nm}$, \triangle) 454 nm , cell with plane-parallel faces; \times) $\lambda_0 = 515 \text{ nm}$, cell with hemisphere. The dashed lines correspond to isotropy of the local-field tensor f .

$\langle P_2 \rangle$ and $\langle P_4 \rangle$ remain practically unchanged within the limits of experimental accuracy.

Thus, in the case of objects similar to the one considered here, allowance for the anisotropy of the tensor f is more important than the variation of R on going from the isotropic to the nematic phase. This conclusion cannot be extended, however, to cases in which the condition $R \ll 1$ is violated. In particular, such a situation is possible for end groups. As seen from Fig. 4, the values of $\langle P_4 \rangle$ are not small compared with $\langle P_2 \rangle$, so that the additional terms of the expansion of (1) are needed for a more exact simulation of the function $F(\theta)$.

- ¹B. K. Vainshtein and I. G. Chistyakov, Problemy sovremennoy kristallografii (Problems of Modern Crystallography), Nauka, 1975, pp. 12–26.
- ²P. G. de Gennes, The Physics of Liquid Crystals, Oxford Univ. Press, 1974.
- ³B. K. Vainshtein and I. G. Chistyakov, Dokl. Akad. Nauk SSSR **153**, 326 (1963) [Sov. Phys. Dokl. **8**, 1044 (1964)].
- ⁴I. Chistyakov, Adv. in Liq. Cryst., New York, **1**, 143 (1975).
- ⁵L. M. Blinov, Elektro- i magnitooptika zhidkikh kristallov (Electro- and Magneto-optics of Liquid Crystals) Nauka, 1978.
- ⁶S. Jen, N. A. Clarc, and P. S. Pershan, J. Chem. Phys. **66**, 4635 (1977).
- ⁷P. J. Collings, T. J. McKee, and J. R. McColl., J. Chem. Phys. **65**, 3520 (1976).
- ⁸E. M. Aver'yanov and V. F. Shabanov, Preprint Inst. Fiz. CO Akad. Nauk SSSR No. 65F, Krasnoyarsk, 1977.
- ⁹A. V. Tolmachev, V. G. Tishchenko, and L. N. Lisetskii, Fiz. Tverd. Tela (Leningrad) **19**, 1886 (1977) [Sov. Phys. Solid State **19**, 1105 (1977)].
- ¹⁰V. K. Dolganov, Fiz. Tverd. Tela (Leningrad) **18**, 1786 (1976) [Sov. Phys. Solid State **18**, 1042 (1976)].
- ¹¹J. P. Heger, J. Phys. (Fr.) Lett. **36**, 209 (1975).
- ¹²A. F. Bunkin, S. G. Ivanov, N. I. Koroteev, A. V. Rezov, and M. L. Sabaeva, Vestn. Mosk. Univ. Fiz. Astron. **18**, 35 (1977).
- ¹³B. K. Vainshtein, E. A. Kosterin, L. M. Kamenchuk, and G. N. Tishchenko, Abstracts of Papers of Fourth All-Union Conf. on Liquid Crystals, Ivanovo, 1977, p. 9.
- ¹⁴K. Miyano, Phys. Lett. A **63**, 37 (1977).

- ¹⁵E. M. Aver'yanov and V. F. Shabanov, *Kristallografiya* **23**, 320 (1978) [*Sov. Phys. Crystallogr.* **23**, 177 (1978)].
- ¹⁶E. M. Aver'yanov and V. F. Shabanov, *Kristallografiya* **23**, 930 (1978) [*sic*].
- ¹⁷V. M. Agranovich, *Usp. Fiz. Nauk* **112**, 143 (1974) [*Sov. Phys. Usp.* **17**, 103 (1974)].
- ¹⁸V. P. Spridonov, Author's Abstract of Candidate's Dissertation, Inst. Foz. CO Akad. Nauk SSSR, Krasnoyarsk, 1977.
- ¹⁹G. Placzek, *Rayleigh and Raman Scattering*, Lawrence Rad. Lab., Univ. of Calif., Livermore, 1959 (transl. from *Handbuch der Radiologie*, 1934. Russ. Transl., ONTI, 1935).
- ²⁰L. N. Ovander, Yu. G. Pashkevich, and N. S. -S. Tyu, in:

- Teoreticheskaya spektroskopiya (Theoretical Spectroscopy)* *Izv. Aka. Nauk SSSR*, 1977, p. 251.
- ²¹V. F. Shabanov, E. M. Aver'yanov, P. V. Adomenas, and V. P. Spiridonov, Preprint Inst. Fiz. CO Akad. Nauk SSSR No. 79F, Krasnoyarsk, 1978.
- ²²M. M. Sushchinskiĭ, *Spektry kombinatsionnogo rasseyaniya molekul i kristallov (Raman-Scattering Spectra of Molecules and Crystals)*, Nauka, 1969.
- ²³P. Chatelain, *Bull. Soc. Fr. Miner.* **66**, 105 (1943).
- ²⁴G. Labrune and M. Bresse, *C. R. Acad. Sci. B* **276**, 647 (1973).

Translated by J. G. Adashko

Disordered Ising model at low temperatures

I. F. Lyuksyutov

L. D. Landau Institute of Theoretical Physics, Academy of Sciences, USSR

(Submitted 27 June 1978)

Zh. Eksp. Teor. Fiz. **75**, 1935-1942 (November 1978)

An Ising model with randomly distributed ferro- and anti-ferromagnetic bonds is treated. A procedure is derived for systematic expansion of the thermodynamic potential at low temperatures, in an arbitrary magnetic field, as a power series in the concentration of antiferro- or ferromagnetic bonds. It is shown that the susceptibility diverges as $1/T$ at $T \rightarrow 0$. The ground-state energy, the magnetic moment, and the residual entropy are calculated as power series in the concentration.

PACS numbers: 75.10.Hk

1. INTRODUCTION

This paper treats the low-temperature behavior of an Ising model with randomly distributed ferro- and antiferromagnetic bonds, equal in absolute value. The treatment is carried out in the case of a square lattice. The method of calculation for a cubic lattice is completely equivalent, and the physical behavior is the same as in the two-dimensional case. The calculation procedure suggested enables one to obtain, in a systematic manner, an expansion of the thermodynamic potential as a power series in, for example, the concentration c of antiferromagnetic bonds in a ferromagnetic matrix:

$$\Phi(J, T, h, c) = \Phi_0 + \Phi_1(J, T, h)c + \Phi_2(J, T, h)c^2 + \dots \quad (1)$$

Here J is the absolute value of the interaction constant, T is the temperature, and h is the magnetic field. The functions Φ_1 , Φ_2 , etc. are calculated to within terms of order $e^{-2J/T}$, i.e., for the case of low temperatures.

In order to obtain the result, one first performs a dual transformation of the partition function in an arbitrary magnetic field. Then, by a procedure that reduces to the enumeration of a certain number of graphs, one calculates successively the functions Φ_1 , Φ_2 , etc. This enables one to calculate the energy of the ground state, the entropy, the magnetic moment, and the susceptibility.

2. DUAL TRANSFORMATION

The Hamiltonian of the model under consideration, for a square lattice, has the form

$$H = - \sum_{i,j} \{ J_{i+\eta_j, j} \sigma_{i,j} \sigma_{i+\eta_j, j} + J_{i, j+\eta_i} \sigma_{i,j} \sigma_{i, j+\eta_i} + h \sigma_{i,j} \}. \quad (2)$$

Here the indices i and j enumerate the sites of the square lattice along the horizontal and vertical directions respectively; $\sigma_{i,j}$ is the spin variable ($\sigma_{i,j} = \pm 1$); and $J_{i+\eta_j, j}$ is the interaction constant. It is assigned on the edges of the lattice cells and is numbered according to the coordinates of their centers. If c is, for example, the concentration of antiferromagnetic bonds in a ferromagnetic matrix, then the interaction constant has the value $+J$ with probability $1-c$ and the value $-J$ with probability c .

The partition function corresponding to (2) can be represented in the following form (N is the number of lattice sites):

$$Z = ch^{2N} (J/T) \text{ch}^N (h/T) \sum_{\sigma=\pm 1} \prod_{i,j} (1 + \text{th}(J_{i+\eta_j, j}/T) \sigma_{i,j} \sigma_{i+\eta_j, j}) \times (1 + \text{th}(J_{i, j+\eta_i}/T) \sigma_{i,j} \sigma_{i, j+\eta_i}) (1 + \text{th}(h/T) \sigma_{i,j}). \quad (3)$$

After summation over all values of σ , there will remain on the right side of (3) a sum over all possible products of factors $\tanh(J_{i+\eta_j, j}/T)$ and $\tanh(h/T)$. It